Supporting Information

Soft Phonon Modes from Off-center Ge atoms Lead to Ultralow Thermal Conductivity and Superior Thermoelectric Performance in n-type PbSe-GeSe

Zhong-Zhen Luo,[1,2] Shiqiang Hao,[3] Xiaomi Zhang,[3] Xia Hua,[3] Songting Cai,[2,3] Gangjian Tan,[2] Trevor P. Bailey,[4] Runchu Ma,[4] Ctirad Uher,[4] Chris Wolverton,[3] Vinayak P. Dravid,[3] Qingyu Yan,[1,*] Mercouri G. Kanatzidis[2,*]

[1]School of Materials Science and Engineering, Nanyang Technological University, 50 Nanyang Avenue 639798, Singapore

[2]Department of Chemistry, Northwestern University, Evanston, Illinois 60208, United States

[3]Department of Materials Science and Engineering, Northwestern University, Evanston, Illinois 60208, United States

[4]Department of Physics, University of Michigan, Ann Arbor, Michigan 48109, United States

Corresponding author: alexyan@ntu.edu.sg; m-kanatzidis@northwestern.edu

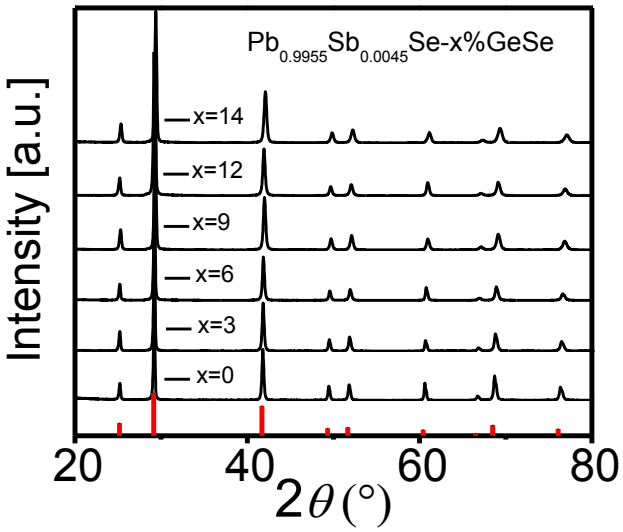

Figure S1. PXRD patterns of $Pb_{0.9955}Sb_{0.0045}Se$-x%GeSe (x = 0, 3, 6, 9, 12 and 14) samples, with all peaks indexed by the PbSe cubic phase (JCPDS #06-0354, red patterns).

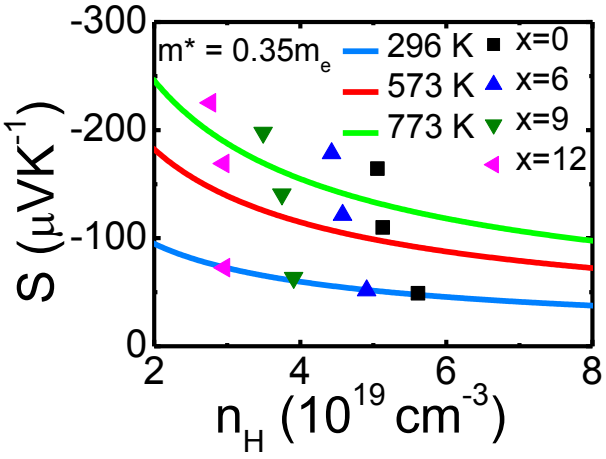

Figure S2. Seebeck coefficient as a function of Hall carrier concentration with an effective mass of 0.35 m_e for $Pb_{0.9955}Sb_{0.0045}Se$-x%GeSe (x = 0, 6, 9 and 12). The solid curves are the theoretical Pisarenko plots at 296 K (cyan), 573 K (red) and 773 K (green) for n-type PbSe with effective mass of electrons of 0.35 m_e.

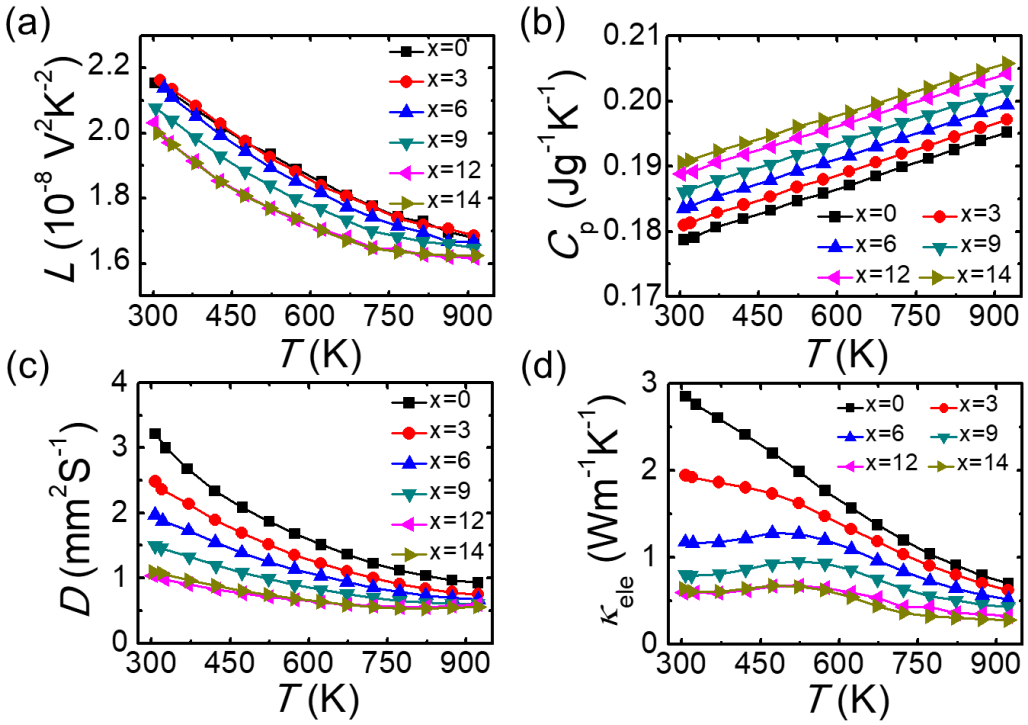

Figure S3. Temperature-dependent (a) Lorenz numbers, L; (b) Heat capacities, C_p; (c) Thermal diffusivity, D; and (d) Electronic thermal conductivity, κ_{ele} for $Pb_{0.9955}Sb_{0.0045}Se$-x%GeSe.

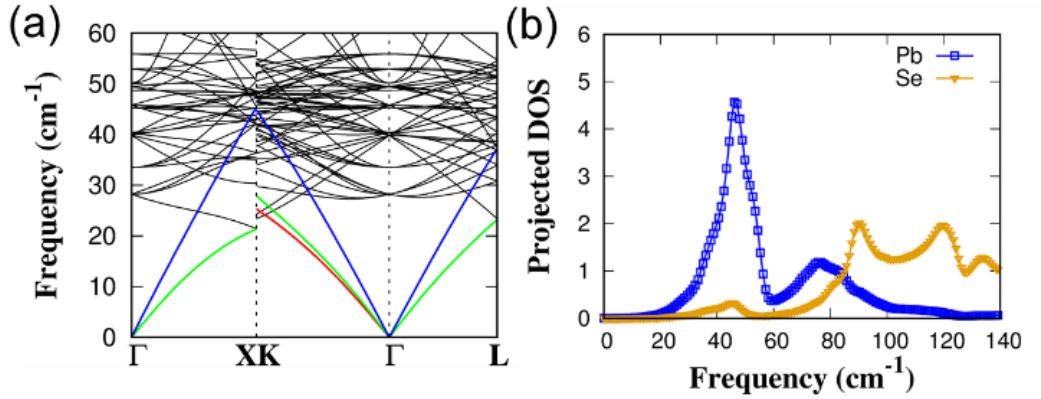

Figure S4. (a) Phonon dispersion curves and (b) the projected phonon density of states (PDOS) for pure PbSe.

In the Debye-Callaway model, we add defect scatterings for longitudinal and transverse modes[S1]

$$\tau_I^L(x)^{-1} = \frac{Vk_B^4\Gamma}{4\pi\hbar^4 v_L^3}x^4T^4 \text{ and } \tau_I^T(x)^{-1} = \frac{Vk_B^4\Gamma}{4\pi\hbar^4 v_T^3}x^4T^4$$

where $\Gamma = \sum_i c_i\left[\frac{m_i - m_{avg}}{m_{avg}}\right]^2$, m_i is the atomic mass of the *i*th defect, $m_{avg} = \sum_i c_i m_i$ is the average atomic mass in the system with different concentration c_i, $x = \frac{\hbar\omega}{k_B T}$, T temperature and $v_{L,}v_T$ the longitudinal and transverse phonon velocities, respectively. The effects of Ge alloying on suppressing κ_{lat} is shown in the below figure:

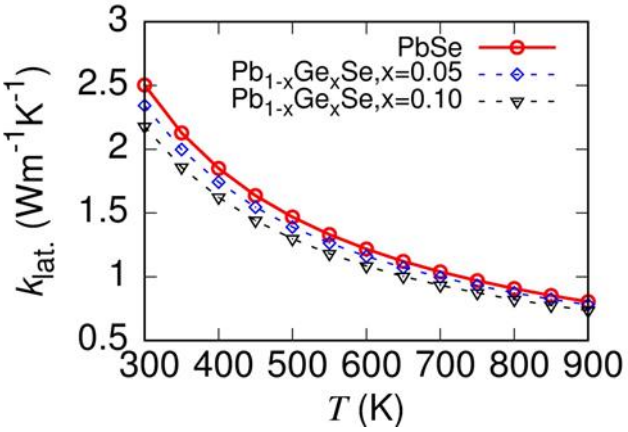

Figure S5. Lattice thermal conductivity comparison of pure PbSe and with 5% and 10% Ge-alloyed samples without accounting for the off-centering Ge^{2+} defect. The effects on the thermal conductivity are small.

At 300 K, κ_{lat} decreases from around 2.5 $Wm^{-1}K^{-1}$ to 2.36 $Wm^{-1}K^{-1}$ with 5% Ge and 2.27 $Wm^{-1}K^{-1}$ with 10% Ge alloying. Evidently, the Ge alloying effect on the lattice thermal conductivity through mass fluctuation is not as significant as the impact of the off-centering defect that induces diminished phonon vibration frequencies and phonon velocities. Thus, the main cause of the κ_{lat} decrease by Ge alloying originates from the Ge off-centered atomic structure. The off-centered Ge induces local lattice strain that lowers the acoustic phonon frequencies, velocities and Debye temperature yielding a decrease in κ_{lat} by 26% of lattice thermal conductivity relative to the pure PbSe calculated (Debye-Grüneisen) value at 300 K. On the other hand, at high concentration (10%) of Ge impurities, the phonon-impurity scattering decreases κ_{lat} by 9% of pure PbSe κ_{lat} value at 300 K as shown in Figure S5. The off-centered Ge also induces softening of the low-lying optical phonon modes, and may cause a further decrease in the lattice thermal conductivity, but this contribution is not included in our Debye Grüneisen calculations. All these combined effects help to understand the experimental observation of κ_{lat} decrease by 50% of κ_{lat} by 12% of Ge alloying.

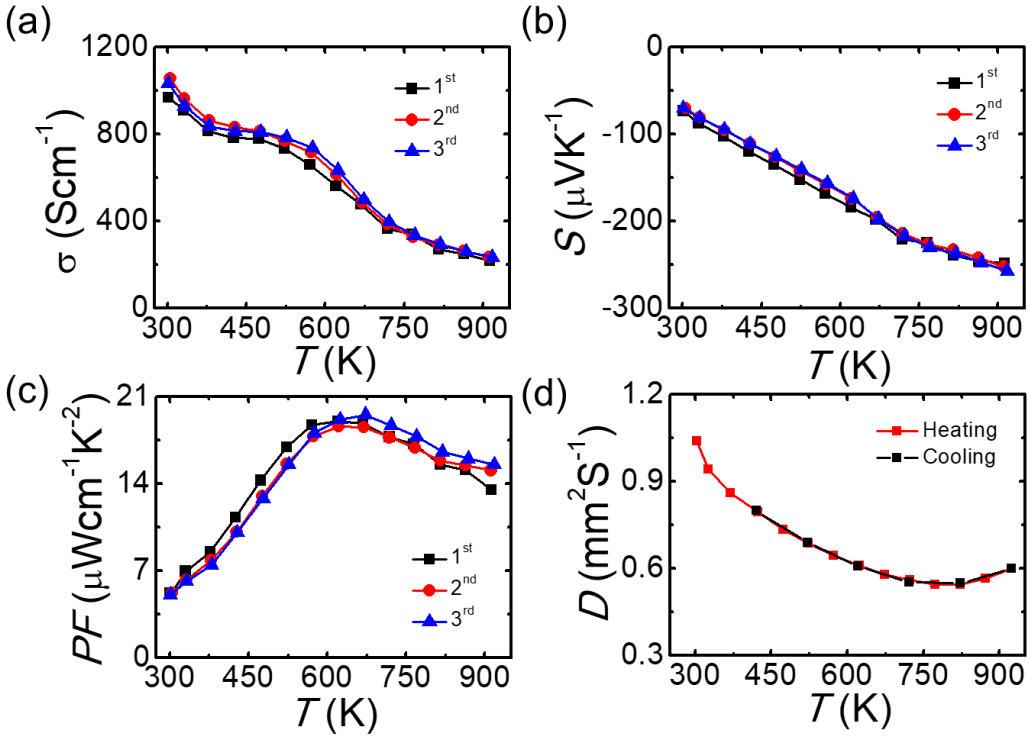

Figure S6. The $Pb_{0.9955}Sb_{0.0045}Se$-12%GeSe sample was measured 3 times with almost no changes in the (a) Electrical conductivity, σ; (b) Seebeck coefficient, S; and (c) Power factor, PF, showing the good repeatability and stability. Moreover, thermal diffusion coefficient, D (d) also displays the good repeatability during heating and cooling processes.

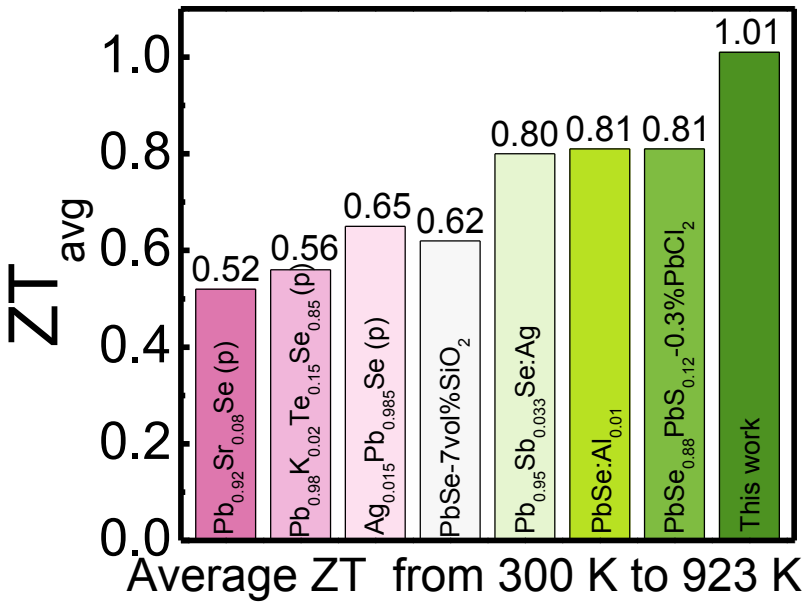

Figure S7. Comparison of the average thermoelectric figure of merit, ZT_{avg}, values with the temperature gradient of 300 K to 923 K for several n- and p-type PbSe-based thermoelectric materials.[S2-8]

Table S1. Room temperature densities of $Pb_{0.9955}Sb_{0.0045}Se$-x%GeSe (x = 0, 3, 6, 9, 12 and 14)

Composition	Measured Density, gcm^3	Theoretical Density,* %
$Pb_{0.9955}Sb_{0.0045}Se$	8.17	98.9
$Pb_{0.9955}Sb_{0.0045}Se$-3%GeSe	8.09	98.9
$Pb_{0.9955}Sb_{0.0045}Se$-6%GeSe	7.97	98.4
$Pb_{0.9955}Sb_{0.0045}Se$-9%GeSe	8.01	99.5
$Pb_{0.9955}Sb_{0.0045}Se$-12%GeSe	7.76	97.5
$Pb_{0.9955}Sb_{0.0045}Se$-14%GeSe	7.7	97.6

References

S1. D. T. Morelli, J. P. Heremans and G. A. Slack, *Phys. Rev. B*, 2002, **66**, 195304.

S2. Q. Zhang, F. Cao, W. Liu, K. Lukas, B. Yu, S. Chen, C. Opeil, D. Broido, G. Chen and Z. Ren, *J. Am. Chem. Soc.*, 2012, **134**, 10031-10038.

S3. J. Androulakis, I. Todorov, J. He, D.-Y. Chung, V. Dravid and M. Kanatzidis, *J. Am. Chem. Soc.*, 2011, **133**, 10920-10927.

S4. Q. Zhang, H. Wang, W. Liu, H. Wang, B. Yu, Q. Zhang, Z. Tian, G. Ni, S. Lee, K. Esfarjani, G. Chen and Z. Ren, *Energy Environ. Sci.*, 2012, **5**, 5246-5251.

S5. H. Wang, Z. M. Gibbs, Y. Takagiwa and G. J. Snyder, *Energy Environ. Sci.*, 2014, **7**, 804-811.

S6. S. Wang, G. Zheng, T. Luo, X. She, H. Li and X. Tang, *J. Phys. D: Appl. Phys*., 2011, **44**, 475304.

S7. C.-F. Wu, T.-R. Wei, F.-H. Sun and J.-F. Li, *Adv. Sci.*, 2017, **4**, 1700199.

S8. Z. Chen, B. Ge, W. Li, S. Lin, J. Shen, Y. Chang, R. Hanus, G. J. Snyder and Y. Pei, *Nat. Commun.*, 2017, **8**, 13828.